SAND2002-2908P

Direct magnetic implosion experiments on Z

S. A. Slutz, D.M. Sinars, and D. Bliss
Sandia National Laboratories

Abstract

The critical mass of fissile materials can be reduced substantially by compression. Small fission explosions could be used for an inherently safe fission reactor or to power a space-craft. 1-D numerical simulations of this magnetic compression indicate sufficient compression to yield a critical mass of less than 10 g with a driving current of approximately 80 MA. Multidimensional effects will undoubtedly increase the current requirement. We have designed an experiment experiment at the lower current (~20 MA) that is presently available on the Z machine to test the feasibility of direct magnetic compression. Details of the experiment including the proposed diagnostics are given.

I. Introduction

Pulsed power technology is capable of delivering very high currents. The present Z accelerator has a peak current of approximately 20 MA, which is delivered in 100 ns. This current can be used to generate very high pressures. As an example, 20 MA with a pinch radius of 3 mm results in a magnetic pressure of approximately 7 Mbar. These high pressures suggest that one could compress fissile material and thus reduce the critical mass. The reduction in the critical mass occurs because it is the product ρr that determines the probability that a neutron will produce a fission event. A solid spherical assembly of Pu will be critical when $\rho r \sim 100$ g/cm^2. At normal density (19.3 g/cc) this corresponds to a mass of approximately 11 kg. The critical mass scales as ρ^{-2} therefore the critical mass could be reduced to ~10 grams if the material could be compressed to approximately 30 times normal density. Fissile materials such as curium require a smaller ρr due to a larger fission cross section and small neutron absorption cross section. Calculations indicate that criticality is obtained for $\rho r \sim 30$ g/cm^2.

II. The Implosion Simulations

The maximum compression can be obtained in spherical geometry. A z-pinch can provide an almost spherical implosion ("quasi-spherical") by appropriately tayloring the thickness of the shell and using conical electrodes, We used a 2-D MHD code driven by an external circuit with parameters scaled up from the Z accelerator to study these implosions. To simplify the simulations only a small region near the equator was simulated thus making the simulation essentially 1-D. Since we did not have the equation of state for exotic fissile materials such as curium, we used lead as a surrogate material since its initial density is similar. We define the initial aspect ratio as the ratio of the outer

radius of the capsule over the wall thickness of the shell. A number of simulations were performed to determine the peak current needed to drive an implosion to a final 50 g/ cm^2, which should be sufficient to insure prompt criticality of materials such as curium. It was found that the peak current was minimal for an $A_R \sim 5$. A summary of the results for $A_R=5$ is given in Table 1.

Table 1:

mass g	Initial radius	Current MA	Risetime μs	Implosion Velocity cm/μs	Kinetic Energy MJ	CR
5	0.64	81	0.36	2.7	1.8	13.7
10	0.8	81	0.44	2.0	2.0	9.3
20	1.0	78	0.59	1.4	2.0	6.2
40	1.27	70	1.15	1.0	2.0	4.5
80	1.6	63	2.7	0.6	1.5	4.1

The mass of the shell is computed assuming an electrode cone angle of 45 degrees. The results indicate that the required peak current is a fairly weak function of the mass of the shell. This may seem surprising at first since the larger mass shells need less compression. However, the increased initial radius of the larger mass shells decreases the magnetic pressure for a given current and the two effects nearly cancel. The appropriate rise time of the current pulse is a strong function of the shell mass. The implosion velocity is a strong function of the shell mass, but the kinetic energy is nearly constant. The convergence ratio, CR, is defined as the peak average density normalized to the initial solid density. As can be seen the convergence ratio decreases with shell mass as expected.

There are several idealizations to these simulations tending to make them optimistic. Z pinches are known to be Rayleigh-Taylor unstable. The small aspect ratio and the material strength of these shells should make then fairly insensitive to this instability. 2-D numerical simulations of z pinches have been performed but ab initio pinch calculations that accurately predict the effect of the RT instability are not yet possible. Therefore we have designed experiments that can be performed on the existing Z accelerator to determine how closely 1-D simulations predict actual pinch performance.

II. Experimental Design

To keep the initial experiments as simple as possible, we chose simple cylindrical liners. We also wish to choose materials that are easy to machine and do not pose health risks. The implosion depends on the material conductivity and equation of state (EOS). We plan to use aluminum and gold for the first experiments because they are good conductors and there is data on their conductivity and EOS. We found that the implosion

time matched the current profile of the Z accelerator for an aluminum shell with an outer radius of 2.42 mm and an initial aspect ratio of 3. This will be used for the first and third shots, because the lower opacity increases the chance of obtaining useful information with the back lighter. We also want to study the implosion of a gold shell which is more representative of a fissile material. We found that a gold cylinder with an initial outer radius of 2 mm and an aspect ratio of 10 has an implosion time which is nearly the same as the aluminum cylinder. We have designed the two cylinders to have the same implosion time to simplify diagnostic timing.

The monochromatic laser backlighter generating 1.8 keV photons should penetrate the low density blow off and give a measure of the actual average density. We have post processed the numerical simulations to determine the radius that would be inferred by this diagnostic. The inferred outer radius is shown in Fig. 1 for simulations of both an aluminum and a gold cylindrical liner. As can be seen the outer radius decreases to a value of about 300 μm for the gold liner and about 200 μm for the aluminum liner. The monochromatic backlighter has a resolution of about 10 μm which is adequate for this measurement.

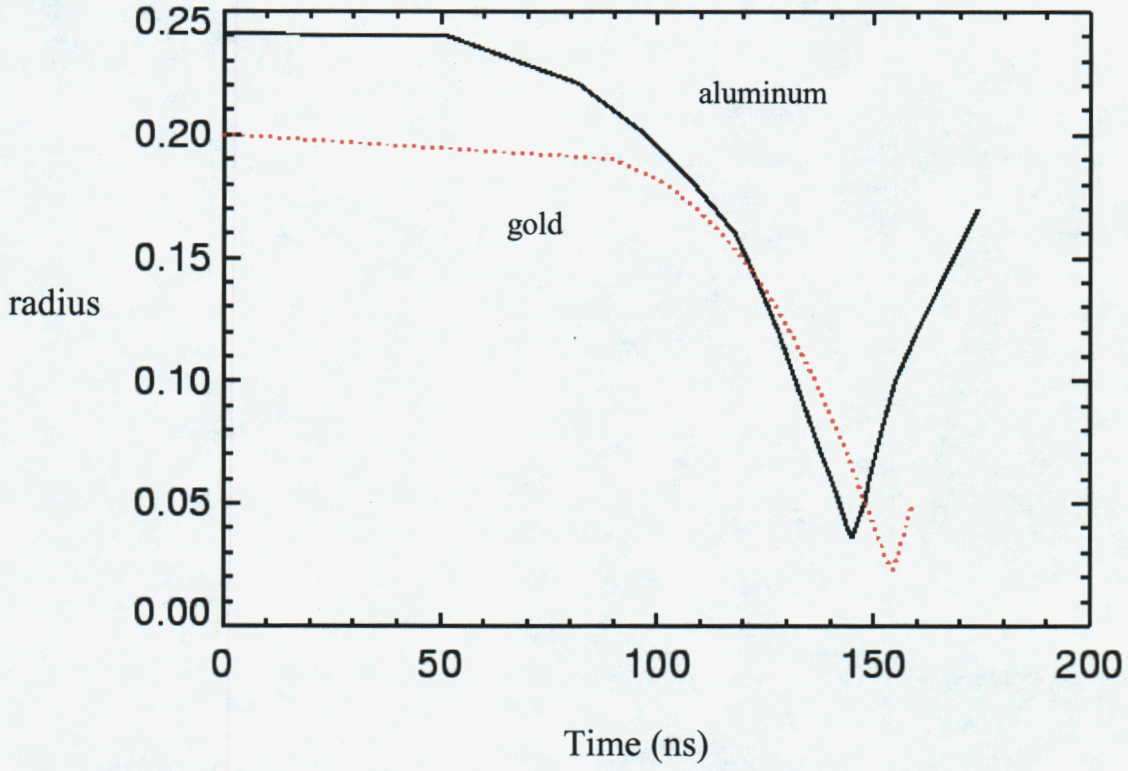

Figure 1 The outer radius as a function of time determine by post processing the numerical simulations assuming a back lighter of 1.8 keV photons

The average density can be determined from the outer radius and the initial mass. This density normalized to the initial solid density is plotted in Fig. 2

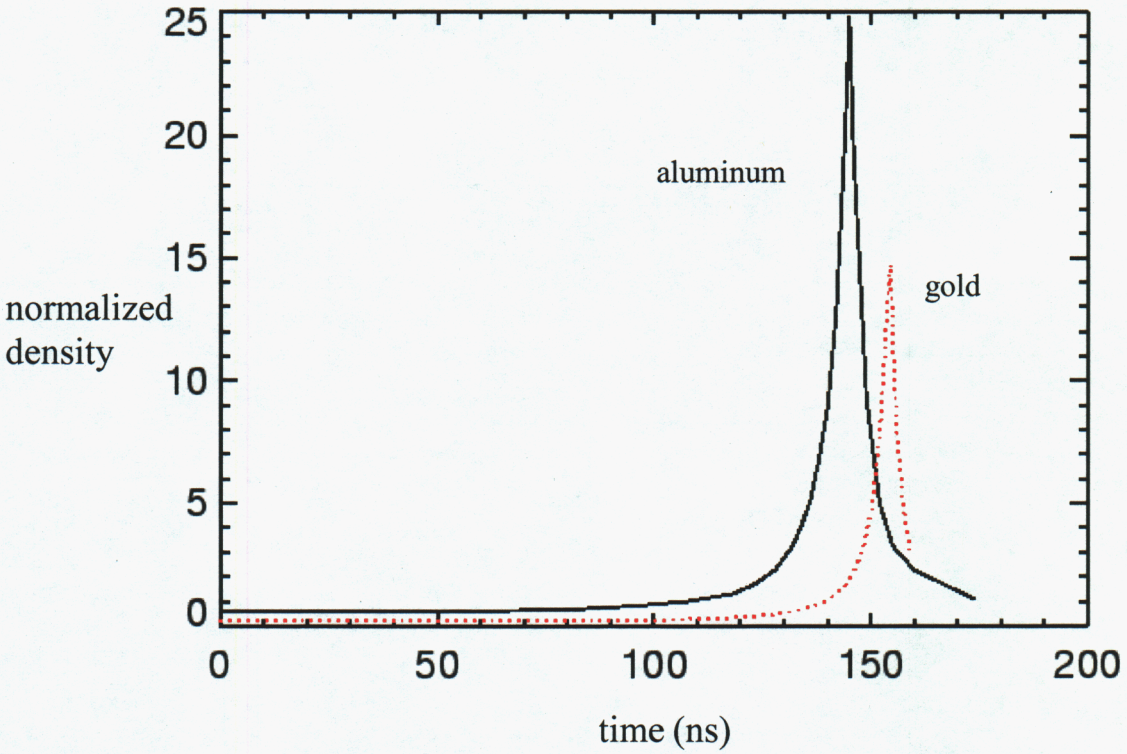

Figure 2 The normalized average density plotted as a function of time

The simulations predict that the aluminum liner will be compressed to almost 25 times solid density, while the gold liner will be compressed to about 14 times solid density. This is because the gold starts off with a higher electron density and the implosion is stopped by the Fermi pressure which is a function of the electron density. Still a compression of 14 would be quite impressive and is larger than the compression needed to reach critical mass for the simulations presented in the last section. Of course the ρr is too small for criticality, but the EOS will have been explored in the appropriate parameter space. Drawings of the hardware design for the aluminum cylinder are shown in Figs. 3 and 4

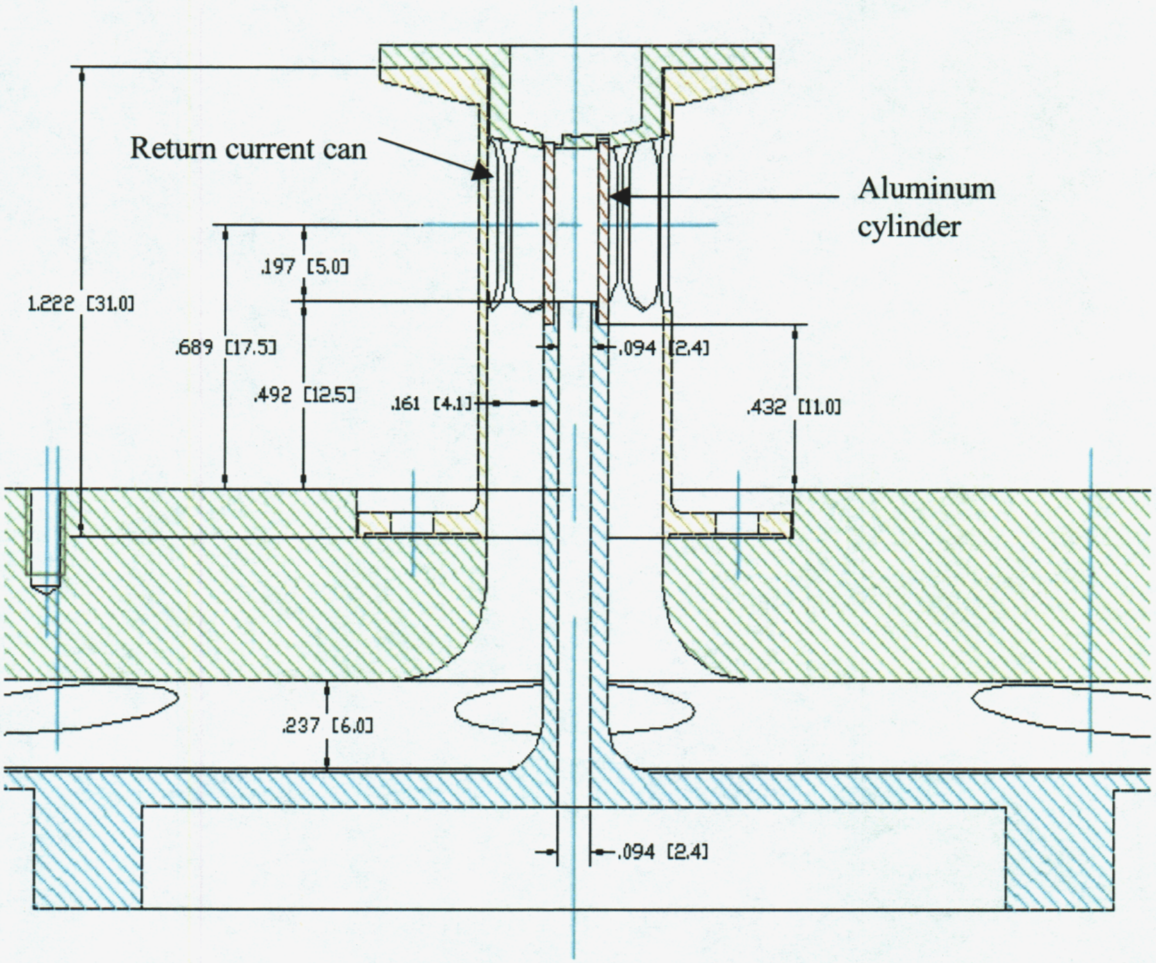

Figure 3 Hardware design for the aluminum cylinder

The pinch has been extended to obtain line of sight access for the backlighter. The return current can has nine slots to allow diagnostic access.

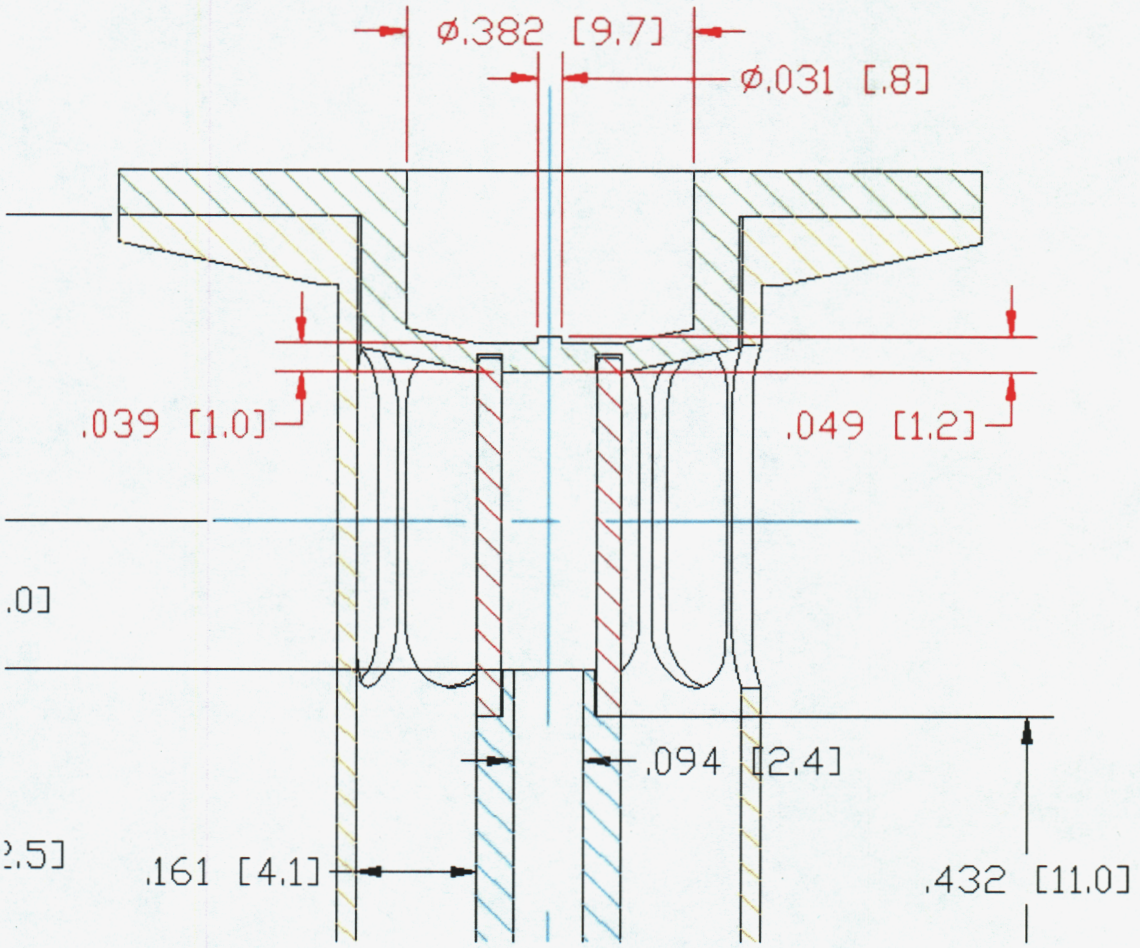

Figure 4 Closup of the hardware design for the aluminum cylinder

The closup view of Fig. 4 shows the stepped top electrode

II. Diagnostics

Monochromatic Backlighter

We plan to carry out these implosion experiments using a laser backlighter as the primary diagnostic. If these implosions are successful, the issue of neutron population must then be addressed. In particular a strong source of neutrons will be needed, since these compressed assemblies will disassemble quickly. The Monochromatic X-ray Backlighting Diagnostic, which uses the Z-beamlet laser. Z-Beamlet, a 2-TW, 2-kJ Nd:glass laser, became operational in 2001 and was used to diagnose high-yield-fusion capsule implosions, driven by wire array z pinches. In these tests the laser beam was focused onto Ti or Fe targets to produce 4.5 or 6.7 keV x rays, respectively, which were used to backlight the capsules in a point-projection geometry. For the point-projection

geometry to succeed, the x-ray background produced by the z pinches had to be eliminated. The soft (<1 keV) x rays were eliminated using filters and hard (>10 keV) x rays were reduced by carefully collimating the detector to a 3 mm field of view centered on a capsule located no closer than 6.5 mm from the ends of either pinch. Simply collimating out the brehmstrahlung-generated hard x rays is not possible when directly imaging the Z-machine, which is the present situation. An alternative is to eliminate the hard x-ray background using spherically bent crystals so only x rays satisfying the Bragg condition, $n\lambda = 2d\sin\theta$, reflect constructively from the surface of the crystal, where λ is the incident photon wavelength, d is the spacing of planes in the crystal, θ is the "grazing" angle (the angle with respect to the crystal plane), and n is an integer corresponding to the crystal reflection order. In this way, both the soft and hard x-ray background from sources within the field of view of the backlighter can be eliminated, and the backlighter system can readily be considered "monochromatic", since it is sensitive to a very narrow band width.

A second advantage of this backlighting geometry is that it can be used to obtain images with <10 μm spatial resolution. For example, a monochromatic backlighting system at the Naval Research Laboratory based on the Si He_α line recently demonstrated 3-5 μm spatial resolution. A third advantage is that the spatial resolution is only weakly dependent on the size of the x-ray source, which means that relatively large sources (>100 μm) can be used. By contrast, to obtain ~10 μm resolution with a point-projection system, the system must either use a small source at low magnification or use a pinhole to reduce the size of the source (at a cost of x-ray flux).

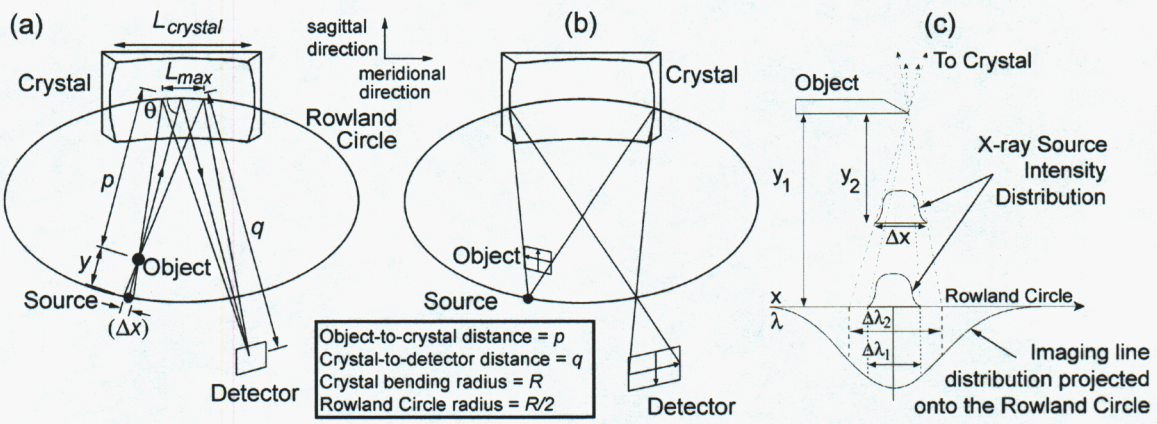

Figure 5. Schematic diagrams illustrating the monochromatic backlighting concept, emphasizing (a) the effect of the source size on the collection angle of the system and (b) the effect of the crystal size in determining the available field of view. If the x-ray source is on the Rowland circle, its width Δx determines the spectral bandpass used for imaging ($\Delta\lambda_1$), which is usually less than the width of the spectral emission line. Moving the source off the Rowland circle can effectively increase the spectral

bandpass of the system as shown to $\Delta\lambda_2$, thereby increasing the efficiency of the system

A operation of an x-ray backlighting system using a spherically bent crystal is shown in Fig. 5. The behavior of this optical system is governed by two general principles: the Bragg condition and the concept of the Rowland circle. The Rowland circle has a radius $R/2$, where R is the bending radius of the crystal. Rays from a point located on the Rowland circle are focused to a corresponding point on the other side of the circle (across the line of normal incidence), as seen in Fig. 5b. Because of the Bragg reflection properties of the crystal, however, only rays from the source satisfying the Bragg condition are focused back onto the Rowland circle. If an object is placed along the path of these rays a distance p from the crystal, where p satisfies

$$R_m \sin\theta > p > (R_m/2) \sin\theta,$$

a detector can be placed at the focal point of the object so that a monochromatic image of the object is obtained.

The focal points for the horizontal (meridional) and vertical (sagittal) planes of the crystal are

$$1/p + 1/q_m = 2/\{R_m \sin\theta\},$$
$$1/p + 1/q_s = \{2\sin\theta\}/R_s,$$

respectively. If $R_s = R_m \sin^2\theta$ (i.e., a toroidally bent crystal is used), then $q_s = q_m$ and astigmatism is reduced to a minimum. Alternatively, $q_s = q_m$ also occurs if $\theta = 90°$. If θ is in the range from 80-90°, however, then a spherical crystal ($R_s = R_m$) can be used with a relatively small amount of astigmatism sufficient to obtain μm-scale spatial resolution. Thus, in this range there is little difference in the performance of spherically and toroidally bent crystals. One can derive the following relationship to determine the object position for a given crystal and desired magnification,

$$p = (R\sin\theta)*(M+1)/(2M).$$

It is not necessary for the backlighting source to lie on the Rowland circle. If the x-ray source is moved inside of Rowland circle the spectral bandwidth and collection solid angle both increase, as illustrated in Fig. 5, making the system more efficient. The penalty is a reduced field of view and worse spatial resolution. Calculations illustrating this are presented elsewhere. This was done with the Mn He_α system to increase the flux at the detector by 17 times.

The field of view of the backlighting system can be estimated by

$$FOV = L_{crystal}*\{y\}/\{p+y\},$$

where $L_{crystal}$ is the width of the crystal in the meridional or sagittal direction and y is the distance from the source to the object. This equation holds for sources both on and inside the Rowland circle.

Table I. A summary of the parameters of the Si He-alpha and Mn He-alpha backlighting systems tested using the Z-Beamlet laser. The bending radius of the crystals was 250 mm.

Emission Line	Si He-alpha	Mn He-alpha
Source Wavlength (angstroms)	6.65	2.016
Crystal	Quartz 10$\underline{1}$1	Quartz 22$\underline{4}$3
Bragg Angle (degrees)	83.9	84.9
Crystal Size (mm)	48 x 11	23 (diam.)
Object to crystal dist. (mm)	145	145
Source to object dist. (mm)	104	40
Field of view (mm)	20 x 5	5 (diam.)
Detector film (Kodak)	RAR 2497	DEF
Laser pulse width (ns)	0.6	1.0
Laser Energy (J)	400-600	1000
Laser spot size (mm)	0.8	0.15

Tests of 1.865 and 6.15 keV monochromatic backlighting systems were carried out in a calibration chamber for the Z-Beamlet laser. The parameters of these test systems, summarized in Table I, were chosen with the backlighting requirements for experiments on the Z-machine in mind. Note that in the Mn He_α system the source was located 63 mm inside the Rowland circle to increase the flux reaching the detector by 17 times.

The object in these experiments was an electroformed Ni mesh with 33.5 μm rectangular wires (5 μm thick) spaced every 318 μm. Sample images from these tests, along with a sample lineout through one wire, are shown in Fig. 6. The Si He_α system was designed for a spatial resolution of about 10 μm, and the Mn He_α system for a spatial resolution of about 6 μm. The experimentally measured spatial resolution varied from 9 to 13 μm for the Si He_α system (center to edge), and from 10 to 12 μm for the Mn He_α system (center to edge).

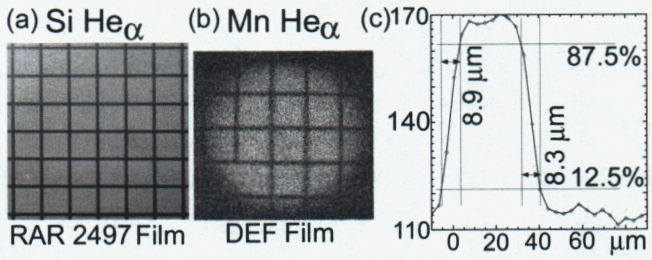

Figure 6 Test images of a 33.5 μm Ni mesh obtained using (a) the Si He_α and (b) the Mn He_α backlighting systems. (c) A sample lineout through a portion of the Ni mesh image in (a).

The first Si He_α tests on the Z machine studied the implosion of cylindrical tungsten wire arrays that were 20 or 12 mm in diameter. Recent work suggests that not all of the mass accelerates to the axis during the implosion, but that some of the mass is "left behind"

near the original location of the wire arrays. One goal of the Si He_α backlighter was to directly measure the presence of any mass left behind. The wire-array hardware for these tests was designed to allow a field of view suitable for such measurements, as depicted in Fig. 7. Though the field of view shown in Fig. 7 extends all the way to the axis of the system, during the experiments a 75 μm Au foil was placed over the inner 2 mm of the exit aperture to prevent x rays from the z pinch from reaching the detector. The detector (film) was placed inside a collimated tungsten/stainless steel housing as shown in Fig. 8. In addition, two tungsten blocks were placed in the direct line-of-sight between the film and the z-pinch source. X rays reflected from the crystal pass through a 2 mm aperture in one of the tungsten blocks, and the line-of-sight between this aperture and the return-current can was blocked using the second tungsten piece.

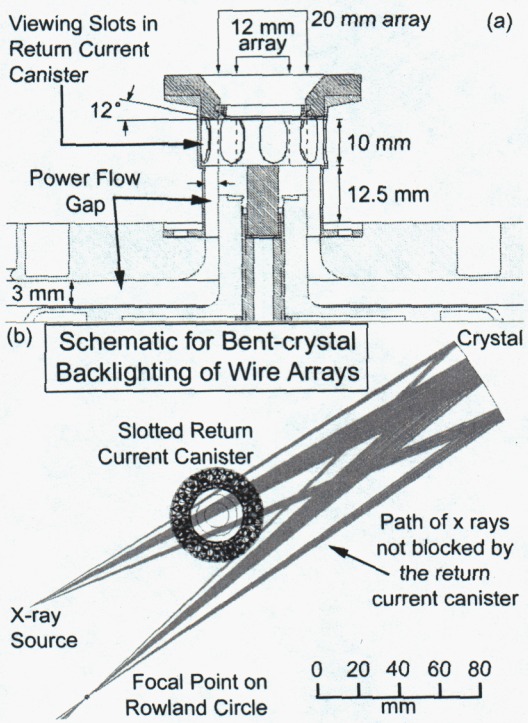

Figure 7 (a) Schematic diagram of the wire-array hardware. In these tests the center of the wire array is 17.5 mm above the horizontal plane to accommodate the existing detector hardware. There are 9 slots in the return-current canister for diagnostic access. Using the ZEMAX ray-tracing program to simulate the Si He_α geometry, the width of the slots was adjusted to obtain the desired field of view of the 20 mm and 12 mm wire arrays being tested. The circles inside the canister in (b) indicate the positions of these arrays.

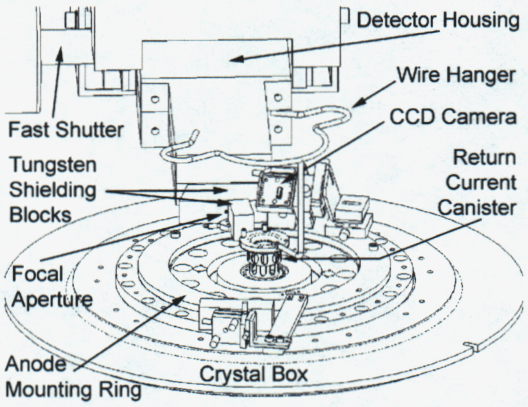

Figure 8 A diagram of the Z-machine hardware for the Si He_α backlighting system. A CCD camera is used to align the focal spot of the laser beam on a target foil (not shown) mounted on the sloped face of the tungsten shielding block. The crystal focuses the source x rays through a 2 mm aperture in one of two tungsten shielding blocks. The second block is used to eliminate the direct line of sight between the return-current can and the aperture. A fast-closing shutter mounted in the detector housing prevents debris from reaching the film.

On July 5, 2002, the Si He_α system was fielded on a Z-machine shot for the first time. The load on this test was a 12 mm diameter, 10 mm tall, 180 W wire array, so only the center image of the object (from r=6 mm to r=2 mm) was expected to contain data. The film from this test is shown in Fig. 9. The image, taken about 36 ns before peak x-ray emission, shows a non-uniform axial and radial mass distribution in the imploding pinch. A detailed analysis of the image is pending.

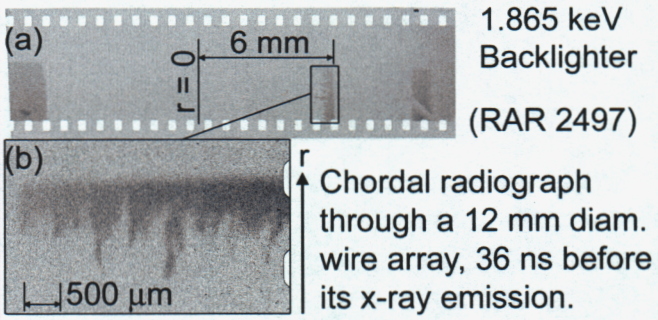

Figure 9 (a) Sample film result from Z-machine test Z931. The load was a 12 mm diameter, 180 W wire array. The image was made 36 ns before the peak z-pinch x-ray emission (b) An expanded view of the central slot image, showing the complex axial and radial mass distribution.

The Si He-alpha (1.865 keV) monochromatic x-ray backlighting system is the primary diagnostic for the upcoming direct magnetic compression experiments. The load hardware for the Z-machine was described in the last section. As in the wire-array experiments described above, the imploding cylinder will be viewed through a slotted return-current canister. This canister will have 9 slots corresponding to each of the nine diagnostic lines of sight on the Z-machine. The design and orientation of the slots is being adjusted to optimize the backlighter view of the compressed cylinder.

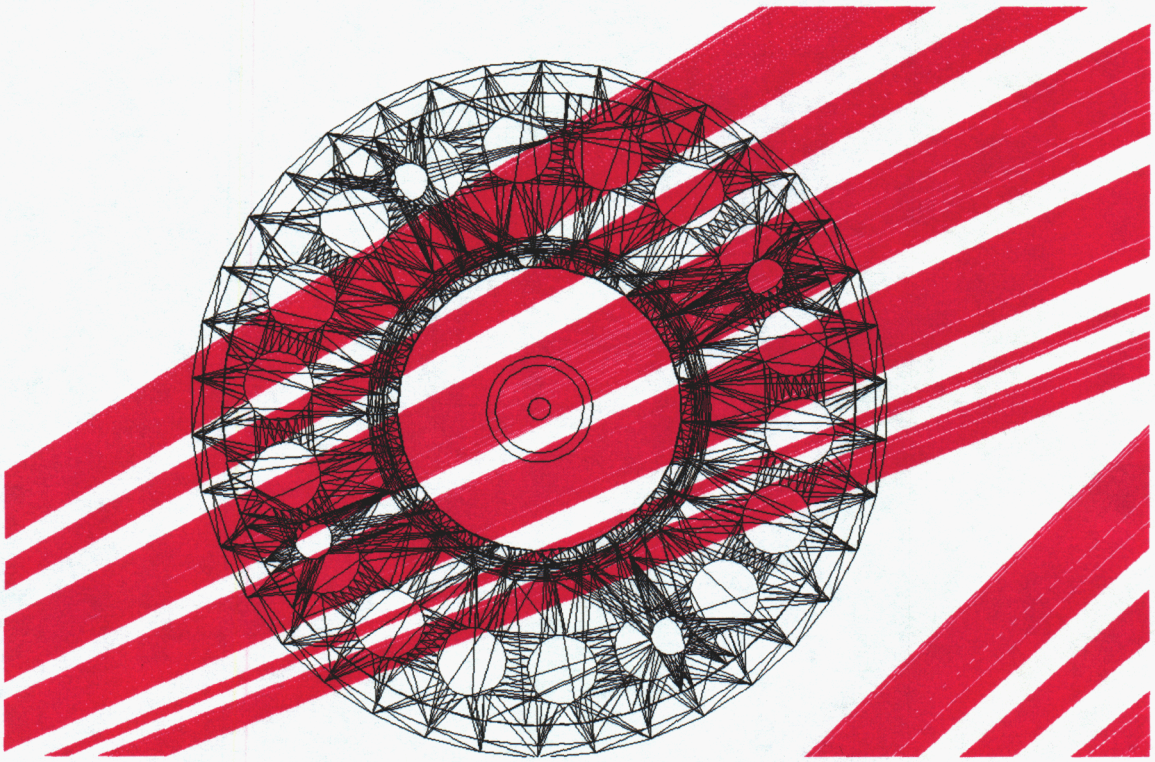

Figure 10 Using the ZEMAX ray-tracing program to simulate the Si He_{α}. The width of the slots was adjusted to obtain the desired field of view of the Al cylinder. The circles inside the canister in indicate the inner and outer walls of the Al cylinder. The innermost circle is a 1 mm diameter fiducial that indicates the approximate size of the cylinder at maximum compression..

In Fig. 10, we present a top-down view of the return-current can and the Al load. A 1 mm diameter circle is also included on the axis to represent the approximate size of the cylinder at maximum compression. The gray lines shown passing through the return-current cylinder show the available field of view for these experiments. This figure indicates that the field of view extends on one side from outside the original location of the Al cylinder down past r=0. The field of view on the other side extends from r=0 to

about r=1 mm, so that if our target goal of about 5 times compression is achieved we will be able to see the entire compressed cylinder.

The success of the Si He-alpha imaging system during previous Z experiments is encouraging for the upcoming direct compression experiments. These experiments are expected to produce less x-ray background than the wire-array experiments, so the backlighting system should be even more reliable. The main experimental issue with this backlighter will be obtaining accurate timing between the Z-Beamlet laser and the cylinder implosion. At present, the Z-Beamlet laser can be synchronized to the Z-machine to within about ±3 ns. Since this load has never been attempted on the Z-machine, there will also be some slight uncertainty in the precise timing of the cylinder implosion. After the first experiment, however, we will be able to quantify the latter timing, so that the subsequent experiments will have more accurate timing.

Active shock breakout

A very large pressure (~ 1×10^{10} atmospheres) is generated when the cylinder implodes on axis. The pressure will send a strong shock wave into the electrodes on the top and bottom of the pinch. We plan to measure the time that this shock waves reaches the upper surface of the top electrode. This is accomplished by irradiating the upper surface of the top electrode with a laser and measuring the reflected light. Since the upper surface of the electrode is polished the reflectivity is high before the arrival of the shock. The arrival of the shock wave at the surface destroys the surface and substantially reduces the reflectivity. This allows us to measure the time of shock breakout. The upper electrode has been designed to have a steps so that the velocity of the shock wave can be determined from the shock breakout time difference. We can then relate these results to the peak pressure through 2-D hydrodynamic simulations

Standard diagnostics

We will image the pinch using CCD x-ray cameras. This will give us an indication of the electrical current path at a time near to peak compression. We will also have the standard array of current monitors to determine the current delivered to the pinch.

References

1 Kathleen S. Holian, "T-1 Handbook of Material Properties Data Bases" Vol. 1c: Equations of State, LA-10160-MS, Los Alamos, 1984.

2 Degnan et al. Phys. Rev. Lett. 74, 98, 1995.

3 Roger Lenard, private communication

4 S. A. Slutz et. al. "Z-pinch driven isentropic compression for inertial fusion", SAND- 98-2269, Jan. 1999.

5 Freeman J. Dyson, Physics Today, Vol. 21, 411968

6 D. L. Peterson, R. L. Bowers, J. L. Brownell, A. E. Greene, K. D. McLenitham, T.